SOFT SWITCHING IN PV GRID CONNECTED INVERTER

A. Mohamed Ithrith*, G. Naveen**, G. Vignesh***
& N. K. Sakthivel****
Department of Electrical and Electronics Engineering, University
College of Engineering, Arni, Tamilnadu

Abstract:
Low leakage current and high efficiency are two key indexes for transformer less PV grid-connected inverter. The Transformer less inverter topologies have superior efficiency thanks to saving transformer, but their semiconductor devices are still on hard-switching state at present. First and foremost, a novel zero current-transition (ZCT) concepts for the single-phase full-bridge transformer less PV grid-connected inverters is presented in this project. Second, the zero-current turn-off for high-frequency main switches of the inverters and the zero-current turn-on for auxiliary switches added are achieved by introducing two resonant tanks. Furthermore, a family of ZCT transformer less grid connected inverters with sinusoidal pulse width modulation is deduced. Especially, taking zero current-transition six-switch full bridge topology (ZCT-H6-I) as an example, its operation principle, soft-switching conditions, duty cycle constraints, and parameter design procedure of the resonant tank are analyzed in detail.
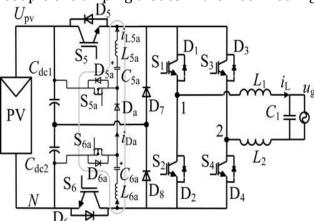
Introduction:

Transformer less PV grid-connected inverters have already found widespread application in practice .The higher conversion efficiency and lower leakage current are two major pushing forces in the development of the transformer less grid-connected inverter. In order to improve the efficiency of the single-phase transformer less grid-connected inverters, two ways are developed: one is constructing multilevel circuit structures (mainly focusing on five-level topologies; and the other is using new semiconductor devices, such as SiC-type or GaN-type devices. The single-phase transformer less multilevel grid-connected inverter has some merits, such as lower voltage stress for power device, smaller filter size and losses, which is beneficial to gain the efficiency. However, the control strategy is sophisticated given the problem of voltage unbalance for the power devices, and the degraded reliability of the inverter.

The wide band gap (WBG) semiconductor devices will promote the development of power electronics and improve on the conversion efficiency essentially. However, at present, the fabricating technique of the new materials stays on immature still, and the rate of finished products is low. Therefore, the cost of the inverter with WBG devices would be increased significantly, which is reverse with the target of "dollar per watt" initial installation cost for PV generation system. Under current technology background, soft-switching technique is a feasible choice to further gain the conversion efficiency for the transformer less PV grid-connected inverter. Adopting soft-switching technique can significantly reduce or, even eliminate the switching losses of Si-semiconductor device; at same time, the rising and falling processes of Si-semiconductor device can be softened to reduce the voltage and current stresses, and electromagnetic interference. Soft-switching technique for dc–ac inverter was first proposed by, which received considerable attention in the past decades. In general, the soft-switching dc–ac inverter can be classified as resonant link dc–ac inverter, resonant transition dc–ac inverter, and load resonant dc–ac inverter, according to their switching characteristics. In addition, according to the position of resonant branches or auxiliary branches added in the inverter topology, the soft-switching topologies can be divided into dc side type, and ac

side type. However, in some topologies, for the drawbacks such as high voltage and current stress, complex control strategy would occur, which make them difficult for industry applications Zero-current-transition (ZCT) technique was initially applied in ac–dc and dc–dc converter ,with the desirable features of pulse width modulation (PWM) and zero-current turn-off for high-frequency switches. Therefore, a simple, efficient ZCT topology for single-phase transformer less PV grid-connected inverter (dc–ac) will be attractive. This paper focuses on improving the conversion efficiency of the transformer less full-bridge topologies by using soft switching means. First, a zero-current-transition H6-I topology (ZCT-H6-I) is proposed, which is derived by reducing the switching losses to gain the conversion efficiency. Compared to hard-switching H6-I topology (HS-H6-I), two ZCT resonant tanks are in parallel added to high-frequency main power devices around, which make the high-frequency main switches running under zero-current turn-off condition. At the same time, the added auxiliary switches can achieve zero-current turn-on. In the proposed ZCT-H6-I, the potential of freewheeling path can also be freely clamped during the freewheeling period, so that the common-mode voltage is constant, which is suitable for transformer less PVgrid-connected applications. Finally, this paper further extends the ZCT concept into other transformer less full-bridge topologies such as Heric, H5, and H6-II; here several typical ZCT-full bridge topologies have been presented. Apparently, the soft-switching technique is a key to gain the conversion efficiency and reduce the cost for PV grid-connected inverters.

Circuit Structure and Operation Principle:

The soft-switching operation for the high frequency main switches S5 and S6 in the HS-H6-I topology, the resonant components C5a , L5a , C6a , L6a, the auxiliary switches S5a , S6a(including their antiparallel diodes or, body diodesD5aand D6a), and one auxiliary diode Da are introduced to form two resonant tanks, L5a= L6a = Lr,and C5a = C6a = Cr. The line-frequency full-bridge inverter consists of the switches S1 , S2 , S3 , and S4 ; the inductors L1 , L2 , and capacitor C1 make up the filter connected to the grid; D7 and D8 are a couple of clamping diodes in the freewheeling period.

All semiconductor devices are ideal switches with antiparallel diodes, and the diodes are also ideal diodes without parasitic parameters (this assumption will ignore the reverse-recovery problem); The capacitance Cdc1 and Cdc2 of the dc filter are large enough to be treated as a constant voltage sources (this assumption will ignore the dc injection problem), and the inductance L1 and L2 of the ac filter are large enough to be treated as a constant current sources at the switching frequency scale. The key operation waveforms of the ZCT-H6-I at the switching frequency scale. The explanation of the key waveforms is as follows: S1,4 , S5,6 , and $S5a,6a$ are the gate driving signals of

S1 and S4 , S5 and S6, S5aand S6a, respectively; iCE5 is the current through the switch S5 ; iD5 is the current through the diode D5 reverse; uS5 is the voltage across the switch S5 ; iDS5a is the current through the switch S5a; iD5ais the current through the diode D5areverse; uS5ais the voltage across the switch S5a ; iDa is the current through the diode Da ; uDa is the voltage across the diode Da ; iS1,S 4 and iD3,D2 are the current through the switches S1 and S4 , and the current through the diodes D3 and D2 , respectively; iL5aand uC5aare the current through the inductor L5aand the voltage across the capacitor C5a , respectively, and ILa and UCa are the peak value of resonant inductor and resonant capacitor, respectively; iLis the current through the inductor L1 , and ILis its amplitude; in positive half cycle of the grid-in current, S1 and S4 are always ON, S2 and S3 are always OFF; in negative half cycle, S1 and S4 are always OFF, S2 and S3 are always ON. S5 and S6 commutate at the high switching frequency with the same commutation orders, the auxiliary switches S5aand S6a, respectively, commutate with S5 and S6 with an overlapping time, and the drive logic timing of all switches is illustrated in Fig. . Obviously, the line-frequency switches S1 – S4 have a little switching loss, and the majority of the switching losses distribute on the high frequency switches S5 and S6. to zero at t1.

Operation Principle Analysis:

Before the analysis, the following assumptions are given: 1) All semiconductor devices are ideal switches with antiparallel diodes, and the diodes are also ideal diodes without parasitic parameters (this assumption will ignore the reverse-recovery problem); 2) the capacitance Cdc1 and Cdc2 of the dc filter are large enough to be treated as a constant voltage sources (this assumption will ignore the dc injection problem), and the inductance L1 and L2 of the ac filter are large enough to be treated as a constant current sources at the switching frequency scale.

The key operation waveforms of the ZCT-H6-I at the switching frequency scale. The explanation of the key waveforms is as follows: S1,4 , S5,6 , and S5a,6aare the gate driving signals of S1 and S4 , S5 and S6, S5aand S6arespectively; iCE5 is the current through the switch S5 ; iD5 is the current through the diode D5 reverse; uS5 is the voltage across the switch S5 iDS5a is the current through the switch S5a ; iD5ais the current through the diode D5areverse; uS5ais the voltage across the switch S5a ; iDa is the current through the diode Da; uDa is the voltage across the diode Da ; iS1,S 4 and iD3,D2 are the current through the switches S1 and S4 , and the current through the diodes D3 and D2 respectively; iL5aand uC5aare the current through the inductor L5a and the voltage across the capacitor C5a, respectively, and ILa and UCa are the peak value of resonant inductor and resonant capacitor, respectively; iLis the current through the inductor L1 , and ILis its amplitude; in positive half cycle of the grid-in current, S1 and S4 are always ON, S2 and S3 are always OFF; in negative half cycle, S1 and S4 are always OFF, S2 and S3 are always ON. S5 and S6 commutate at the high switching frequency with the same commutation orders, the auxiliary switches S5and, respectively, commutate with S5 and S6 with an overlapping time, and the drive logic timing of all switches is illustrated . Obviously, the line-frequency switches S1 – S4 have a little switching loss, and the majority of the switching losses distribute on the high frequency switches S5 and S6. One complete switching cycle can be divided into nine stages; because of the similarity, only the switching modes in the positive half period of the grid-incurrent are described in detail.

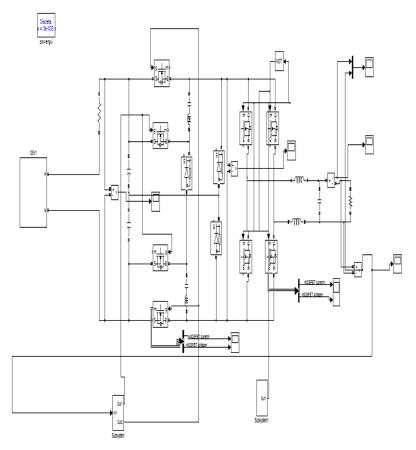**Duty Cycle of High-Frequency and Auxilary Switches:**

Assuming that d1 is the duty cycle of the high-frequency main switches S5 and S6, and d2 is the duty cycle of the auxiliary switches S5aand S6a. Under the conditions

that S5 and S6 are turned OFF at t2 , and S5a and S6aare turned off at t3 , respectively, the overlapping time of the high-frequency main switches and auxiliary switches isΔ = Tr /4, and the duty cycle *d* of the output differential-mode voltage of the ZCT- H6-I is given by
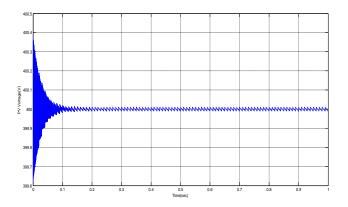
$$d = d1 + d2 - Tr\ 4TS$$

With the assumptions of the grid-in current iL (t) IREFsinω0 tand the modulation signal m = Asin(ω0 t + φ) from the grid-in current controller, the modulation signals of the high frequency main switches and auxiliary switches can be calculated, respectively, In order to guarantee safety of the resonant action, the timing constraint must be satisfied as follows: When the ON time d1TS of the high-frequency main switches is more than a half resonant cycle (Tr/2), the auxiliary switches are initiated to work.
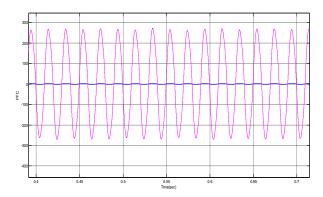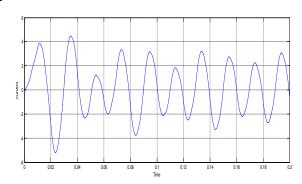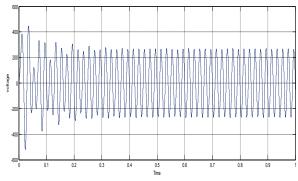
Simulation Diagram:

PV Voltage:

Power Factor Correction:
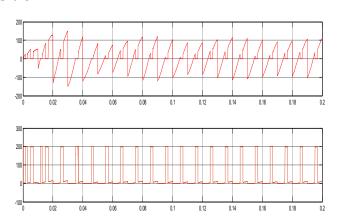

Output Grid Current:

Output Grid Voltage:

Zero Current Transition:

Conclusion:

The soft-switching technology is very important to push the switching frequency into the higher level for PV grid-connected inverter, and the size, weight, and cost can be

reduced significantly. A ZCT concept for transformer less full-bridge topologies has been proposed in this project, which has the following characteristics. 1) The high-frequency main switches realize zero-current turn-off, and the added auxiliary switches realize zero-current turn-on. 2) The ZCT resonant tank has no influence on the differential-mode and common-mode characteristics compared with hard-switching counterpart. It can be concluded that the proposed ZCT concept is suitable for higher power level of single-phase grid-connected systems with solar cell.

Reference:

1. J. F. Gieras and M.Wing, Permanent Magnet Motor Technology—Design and Application. New York, NY, USA: Marcel Dekker, Inc, 2002.
2. C. L. Xia, Permanent Magnet Brushless DC Motor Drives and Controls. Beijing, China: Wiley, 2012.
3. Y. Chen, C. Chiu, Y. Jhang, Z. Tang, and R. Liang, "A driver for the single phase brushless DC fan motor with hybrid winding structure," IEEE Trans. Ind. Electron., vol. 60, no. 10, pp. 4369–4375, Oct. 2013.
4. S. Nikam, V. Rallabandi, and B. Fernandes, "A high torque density permanent magnet free motor for in-wheel electric vehicle application," IEEE Trans. Ind. Appl., vol. 48, no. 6, pp. 2287–2295, Nov./Dec. 2012.
5. X. Huang, A. Goodman, C. Gerada, Y. Fang, and Q. Lu, "A single sided matrix converter drive for a brushless DC motor in aerospace applications, "IEEE Trans. Ind. Electron., vol. 59, no. 9, pp. 3542–3552, Sep. 2012.
6. W. Cui, Y. Gong, and M. H. Xu, "A permanent magnet brushless DC motor with bifilar winding for automotive engine cooling application, "IEEE Trans. Magn., vol. 48, no. 11, pp. 3348–3351, Nov. 2012.
7. C. C. Hwang, P. L. Li, C. T. Liu, and C. Chen, "Design and analysis of a brushless DC motor for applications in robotics," IET Elect. Power Appl., vol. 6, no. 7, pp. 385–389, Aug. 2012.
8. T. K. A. Brekken, H. M. Hapke, C. Stillinger, and J. Prudell, "Machines and drives comparison for low-power renewable energy and oscillating applications," IEEE Trans. Energy Convers., vol. 25, no. 4, pp. 1162–1170, Dec. 2010.
9. N. Milivojevic, M. Krishnamurthy, A. Emadi, and I. Stamenkovic, "Theory and implementation of a simple digital control strategy for brushless DC generators," IEEE Trans. Power Electron., vol. 26, no. 11, pp. 3345–3356, Nov. 2011.
10. T. Kenjo and S. Nagamori, Permanent Magnet Brushless DC Motors. Oxford, U.K.: Clarendon Press, 1985.
11. J. R. Handershot and T. J. E Miller, Design of Brushless Permanent Magnet Motors. Oxford, U.K.: Clarendon Press, 2010.
12. T. J. Sokira andW. Jaffe, Brushless DCMotors: Electronics Commutation and Controls. Blue Ridge Summit, PA, USA: Tab Books, 1989.
13. H. A. Toliyat and S. Campbell, DSP-Based Electromechanical Motion Control. New York, NY, USA: CRC Press, 2004.
14. Limits for harmonic current emissions (equipment input current ≤16 A per phase)," International Standard IEC 61000-3-2, 2000
15. N. Mohan, T. M. Undeland, and W. P. Robbins, Power Electronics: Converters, Applications and Design. New York, NY, USA: Wiley, 2009.
16. B. Singh, B. N. Singh, A. Chandra, K. Al-Haddad, A. Pandey, and D. P. Kothari, "A review of single-phase improved power quality ACDC converters," IEEE Trans. Ind. Electron., vol. 50, no. 5, pp. 962–981, Oct. 2003.

17. B. Singh, S. Singh, A. Chandra, and K. Al-Haddad, "Comprehensive study of single-phase AC-DC power factor corrected converters with high frequency isolation," IEEE Trans. Ind. Inf., vol. 7, no. 4, pp. 540–556, Nov. 2011.
18. S. B. Ozturk, O. Yang, and H. A. Toliyat, "Power factor correction of direct torque controlled brushless DC motor drive," in Proc. 42nd IEEEIAS Annu. Meeting, Sep. 23–27, 2007, pp. 297–304.
19. T. Y. Ho, M. S. Chen, L. H. Yang, and W. L. Lin, "The design of a high power factor brushless DC motor drive," in Proc. Int. Symp. Comput. Consum. Contr., Jun. 4–6, 2012, pp. 345–348.
20. C. H. Wu and Y. Y. Tzou, "Digital control strategy for efficiency optimization of a BLDC motor driver with VOPFC," in Proc. IEEE Energy Convers. Congr. Expo., Sep. 20–24, 2009, pp. 2528–2534.
21. T. Gopalarathnam and H. A. Toliyat, "A new topology for unipolar brushless DC motor drive with high power factor," IEEE Trans. Power Electron., vol. 18, no. 6, pp. 1397–1404, Nov. 2003.
22. V. Bist and B. Singh, "An adjustable speed PFC bridgeless buck-boost converter fed BLDC motor drive," IEEE Trans. Ind. Electron., vol. 61, no. 6, pp. 2665–2677, Jun. 2014.